Comparison of Left Atrial Area Marked Ablated in Electroanatomical Maps with Scar in MRI

BHRIGU R. PARMAR, M.D.,* TYLER R. JARRETT, B.S.,* NATHAN S. BURGON, B.S.,*
EUGENE G. KHOLMOVSKI, PH.D.,* NAZEM W. AKOUM, M.D.,* NAN HU, PH.D.,†
ROB S. MACLEOD, PH.D.,* NASSIR F. MARROUCHE, M.D.,* and RAVI RANJAN, M.D., PH.D.*

From the *Division of Cardiology, CARMA Center; and †Department of Internal Medicine, University of Utah, Salt Lake City, Utah, USA

Electroanatomic Map Overestimates the Ablated Area. *Background:* Three-dimensional electroanatomic mapping (EAM) is routinely used to mark ablated areas during radiofrequency ablation. We hypothesized that, in atrial fibrillation (AF) ablation, EAM overestimates scar formation in the left atrium (LA) when compared to the scar seen on late-gadolinium enhancement magnetic resonance imaging (LGE-MRI).

Methods and Results: Of the 235 patients who underwent initial ablation for AF at our institution between August 2011 and December 2012, we retrospectively identified 70 patients who had preprocedural magnetic resonance angiography merged with LA anatomy in EAM software and had a 3-month postablation LGE-MRI for assessment of scar. Ablated area was marked intraprocedurally using EAM software and quantified retrospectively. Scarred area was quantified in 3-month postablation LGE-MRI. The mean ablated area in EAM was 30.5 ± 7.5% of the LA endocardial surface and the mean scarred area in LGE-MRI was 13.9 ± 5.9% (P < 0.001). This significant difference in the ablated area marked in the EAM and scar area in the LGE-MRI was present for each of the 3 independent operators. Complete pulmonary vein (PV) encirclement representing electrical isolation was observed in 87.8% of the PVs in EAM as compared to only 37.4% in LGE-MRI (P < 0.001).

Conclusions: In AF ablation, EAM significantly overestimates the resultant scar as assessed with a follow-up LGE-MRI. *(J Cardiovasc Electrophysiol, Vol. pp. 1-7)*

atrial fibrillation, magnetic resonance imaging, radiofrequency ablation

Introduction

Atrial fibrillation (AF) is increasingly managed by radiofrequency ablation, in which left atrial tissue is ablated around the pulmonary vein (PV) antra to create scar with a primary goal of electrically isolating the PVs.[1,2] Further ablation to the posterior wall, roof, or septum varies from center-to-center and is largely operator dependent.[3] To guide ablation, preprocedural magnetic resonance angiography (MRA) or computerized tomography angiography is commonly acquired, segmented in an electroanatomic mapping (EAM) system, and merged with real-time left atrial geometry to create a 3D model of the left atrium (LA). Areas of ablation are routinely marked on these merged maps to more accurately deliver contiguous lesion sets and improve procedural success.[4]

Late-gadolinium enhancement magnetic resonance imaging (LGE-MRI) is also increasingly used to visualize postablative scar in the LA.[5-7] Nonconductive scar takes some time to form fully after ablation and, as a result, a blanking period is required between the ablation procedure and accurate assessment of scar using LGE-MRI.[5,8] Several small studies have shown a correlation between the ablation-related LA scar seen on LGE-MRI and clinical outcomes.[9,10]

Peters *et al.* have shown the presence of scar at the ablation sites marked on EAM, yet studies comparing the EAM-recorded ablation tags with the eventual LA scar seen on LGE-MRI are limited.[11] Although electrophysiologists depend heavily on the EAM to guide and track ablation, no study has evaluated the correlation between the ablated areas marked on the EAM during the procedure and the eventual scar area later seen in LGE-MRI.

The purpose of this study was to assess whether intraprocedural EAM ablated area and PV encirclement correlates with 3-month postprocedural LGE-MRI scar area and PV encirclement. We hypothesized that EAM ablated area significantly overestimates the postprocedural LGE-MRI scar in both total endocardial surface area and PV encirclement.

<div style="text-align: center;">

Methods

</div>

Patient Population

Two hundred thirty-five patients underwent initial AF ablation at the University of Utah Hospital between August 2011 and December 2012. Of the 235 patients, 70 patients had a retrievable MRA LA model merged intraprocedurally with an EAM system and a 3-month postablation LGE-MRI. Study variables were collected after approval by the institutional internal review board.

Ablation Procedure

All patients underwent PV antrum isolation with or without additional ablation by 1 of 3 cardiac electrophysiologists at the University of Utah Hospital. Preprocedural MRA was used to generate a LA shell for merge with the LA anatomy in the CARTO EAM system (Biosense Webster, Diamond Bar, CA, USA). Merging of the shell was accomplished by a landmark registration method using intracardiac echocardiography (ICE) and the merge quality was also verified during the procedure. A 3.5-mm irrigated tip ablation catheter (Thermocool, Biosense Webster) and a circular 10-pole mapping catheter (Lasso, Biosense Webster) were advanced transseptally into the LA under ICE and fluoroscopic guidance. Radiofrequency energy was applied circumferentially to the PV antra for all patients with additional application to the posterior wall in a subset of patients. ICE was used to track the ablation catheter tip during the procedure to ensure good catheter tip tissue contact. After the initial ablation, presence of local electrograms was checked by the lasso or ablation catheter and additional ablation was carried out if there was local electrical activity or the PV was not isolated. Operator 1 used 50 W for LA ablations while repositioning the catheter approximately every 5 seconds. Operator 2 used 35 W with catheter repositioning approximately every 10 seconds for most of the ablation and decreased power to 30 W if close to the esophagus as identified with ICE. Operator 3 used 25–30 W to ablate the posterior wall and 30–35 W for the anterior wall, moving the catheter every 10–12 seconds. Operator 3 also used a temperature probe in the esophagus to monitor the temperature.

During radiofrequency energy delivery, ablation tags with an institutional standard 2 mm radius were marked and projected onto the surface of the MRA shell approximately every 5 seconds for operator 1 and every 10 seconds for operators 2 and 3. The Lasso catheter was used to confirm the electrical isolation of PVs.

Quantification of Ablated Surface Area in EAM

Merged LA models with ablation tags from each procedure were retrieved retrospectively from the EAM software using the CARTO Merge Plus module (CARTO, Biosense Webster). Regions of the model surface covered by ablation tags were outlined by 2 blinded experts using the design line tool and surface areas of these regions were measured with the area measurement tool (Fig. 1). Surface area distal to the PV ostia and the section representing the mitral valve were measured and excluded from the total surface area of the model to quantify LA wall area and reduce variability from PV segmentation. Gaps within ablated regions of 0.5 cm^2 or greater were also measured and excluded from regions with ablation tags to more accurately assess the ablated area.
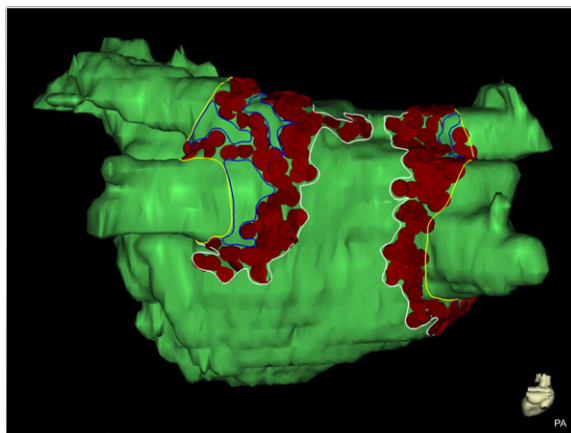
Figure 1. *Measurement of ablated area in EAM. Ablation tags (red) are projected onto the surface of the LA model (green). Lines were drawn on the surface of the model to define the PV ostia (yellow), ablated regions (white), and gaps in ablated regions (blue). Gaps and PV surface area were measured and subtracted from surface area enclosed by white contours to derive ablated surface area. EAM = electroanatomic mapping; LA = left atrium; PV = pulmonary vein.*

Ablated surface areas were then summed and expressed as a percentage of the LA wall area.

In a randomly selected subset of consecutive patients (n = 10), ablation tag size was retrospectively reduced to 1 mm radius to assess for any discrepancy in EAM ablated area and the ablated area was recalculated in EAM using the same process as for 2 mm ablation tag size.

Quantification of Scarred Surface Area from LGE-MRI

All MRI studies were performed on 1.5 or 3 Tesla clinical MR scanners (Siemens Healthcare, Erlangen, Germany). Each LGE-MRI scan was acquired about 15 minutes after contrast agent injection (0.1 mmol/kg, Multihance, Bracco Diagnostic Inc., Princeton, NJ, USA) using a 3D inversion recovery prepared, respiration navigated, electrocardiogram (ECG)-gated, gradient echo pulse sequence using an institutional standard protocol described previously.[12] Typical acquisition parameters were: free-breathing using respiratory and ECG navigation, a transverse imaging volume with acquired voxel size = 1.25 × 1.25 × 2.5 mm (reconstructed to 0.625 × 0.625 × 1.25 mm). The other imaging parameters were optimized for respective field strength of scanner to improve postablation scar visibility and simultaneously keep scan duration acceptable for patients (<15 minutes). For scans performed on 1.5 Tesla scanners, parameters were set as follows: repetition time = 5.4 milliseconds, echo time = 2.3 milliseconds, and flip angle = 20°. For scans performed on 3 Tesla scanner, parameters were: repetition time = 3.1 milliseconds, echo time = 1.4 milliseconds, flip angle = 14°. Depending on subject respiration pattern, typical scan time for the LGE-MRI study on 1.5 Tesla scanner was 8–12 minutes and at 3 Tesla scan time was 5–9 minutes.

Endocardial and epicardial contours were delineated in each slice and assembled in Corview software (Marrek Inc., Salt Lake City, UT, USA) to create a 3D model of the LA. The PVs and the mitral valve were excluded from the segmentation to isolate the LA wall, and the total area of the remaining LA endocardial surface was recorded. Scar was defined using a pixel-intensity threshold algorithm as

TABLE 1
Clinical Characteristics of the Patient Population (n = 70)

Characteristics	Mean ± Standard Deviation
Age (years)	**65.0 ± 2.4**
Body mass index	**31.6 ± 7.2**
	Number (Percent of Population)
Gender	
Male	54 (75.7%)
Female	16 (24.3%)
AF type	
Paroxysmal	34 (48.1%)
Persistent	36 (51.9%)
Permanent	0 (0.0%)
Hypertension	41 (58.6%)
Diabetes mellitus	8 (11.4%)
Obstructive sleep apnea	20 (28.6%)
Coronary artery disease	15 (21.4%)
Congestive heart failure	12 (17.1%)

Figure 2. *Comparison of the mean ablated area along with corresponding standard deviation in EAM and 3-month LGE-MRI for all patients (P < 0.001). EAM = electroanatomic mapping; LGE-MRI = late-gadolinium enhancement magnetic resonance imaging.*

described in previous reports.[9,13,14] In brief, normal and scar tissue were distinguished based on a bimodal distribution of pixel intensities, and scar was defined at 3 standard deviations above the normal mean tissue pixel intensity. With determination of the scar areas, the surface area of the LA endocardial surface covered by enhancement was recorded. Scar area was expressed as a percent of total LA endocardial surface area.

PV Encirclement

Two blinded observers evaluated patterns of ablation in EAM around the PV ostia by estimating the percent of ostial circumference covered by ablation tags in 10% increments. Interobservational consensus was defined as the mean percent of circumference. A disagreement of 20% or greater between observers in circumferential encirclement was resolved with a third observation by a blinded electrophysiologist.

Three blinded observers evaluated scar patterns around the PV ostia in all LGE-MRI segmentations. Each observer estimated the percent of ostial circumference covered by enhancement in increments of 10% and these percentages were averaged to obtain observer consensus. If percent isolation varied by greater than or equal to 20% among the observers, the average of the 2 nearest estimates was used as observer consensus. Complete encirclement was defined as greater than 90% of circumferential coverage of the PV antra by enhancement or ablation tags in both EAM and LGE-MRI.

Statistical Analysis

Paired Student's *t*-test was performed to compare the ablated area in EAM with LGE-MRI scar area as well as percent encirclement of the individual PVs. McNemar's test was applied to compare the number of PVs completely isolated by EAM ablation tags and by LGE-MRI scar. Left or right common PVs were excluded from this analysis. Two-sided P values of less than 0.05 were deemed significant.

Results

Baseline characteristics of the study population are presented in Table 1. The average age was 65 years and 76%
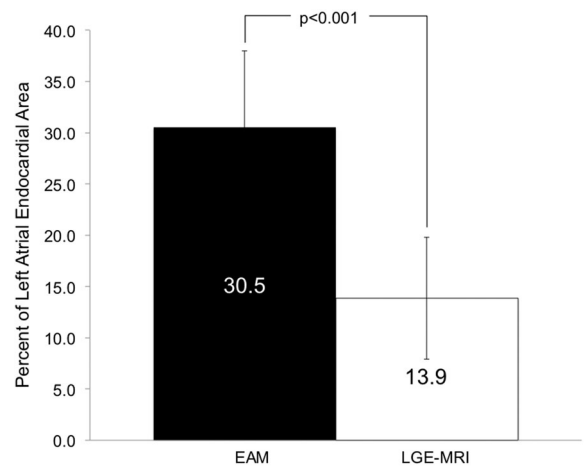
were men. Of the 70 patients, 34 had paroxysmal AF and 36 had persistent AF. Radiofrequency energy was applied circumferentially to the PV antra for all patients (n = 70) with additional application to the posterior wall (n = 38, 54.3%). The mean ablated area as a percent of LA surface area in EAM and the standard deviation was 30.5 ± 7.5%, and the corresponding mean scar area along with standard deviation in LGE-MRI was 13.9 ± 5.9%. The difference between these 2 means was statistically significant (P < 0.001; Fig. 2). Figure 3 shows 2 pairs of EAM and LGE-MRI, one showing a strong correlation between the ablation tags in EAM and the scar from LGE-MRI and the other showing a large discrepancy. The mean total LA surface area and standard deviation were 155.1 ± 36.4 cm^2 in the EAM and 164.5 ± 38.7 cm^2 in the LGE-MRI.

Ablation tag encirclement of the PVs in EAM did not consistently predict scar encirclement in LGE-MRI. While the mean percent of ostial circumference covered by ablation tags in EAM was >90% for all PVs, the corresponding mean in LGE-MRI varied between 70% and 73% with the exception of the left inferior vein that had a mean of 85% (Fig. 4; all P < 0.001). Complete encirclement was significantly more common in EAM compared to LGE-MRI for all 4 PVs (Fig. 5; all P < 0.001). Collectively, 87.8% of all PVs were encircled in EAM compared to 37.4% in LGE-MRI (P < 0.001). Left superior PVs were completely encircled in 74% of the patients in EAM compared to 36% in the LGE-MRI, left inferior PVs were encircled in 86% of the patients in EAM compared to 52% in LGE-MRI, right superior PVs were encircled in 92.6% of the patients in EAM compared to 33.8% in LGE-MRI, and right inferior PVs were encircled in 98.5% of the patients in EAM compared to 27.9% in LGE-MRI (all P values <0.001; Fig. 5).

The number of PVs isolated in any patient was also much higher in EAM compared to LGE-MRI. All 4 PVs were marked isolated in 47% of the patients in EAM compared to only 8.5% based on scar in LGE-MRI. Three veins were isolated in 30% in EAM and 11.4% in LGE-MRI. Two veins were isolated in 21.4% in EAM compared to 12.9% on LGE-MRI. Only 1 vein was isolated in 1.4% of patients in EAM compared to 37% in LGE-MRI and finally there were no
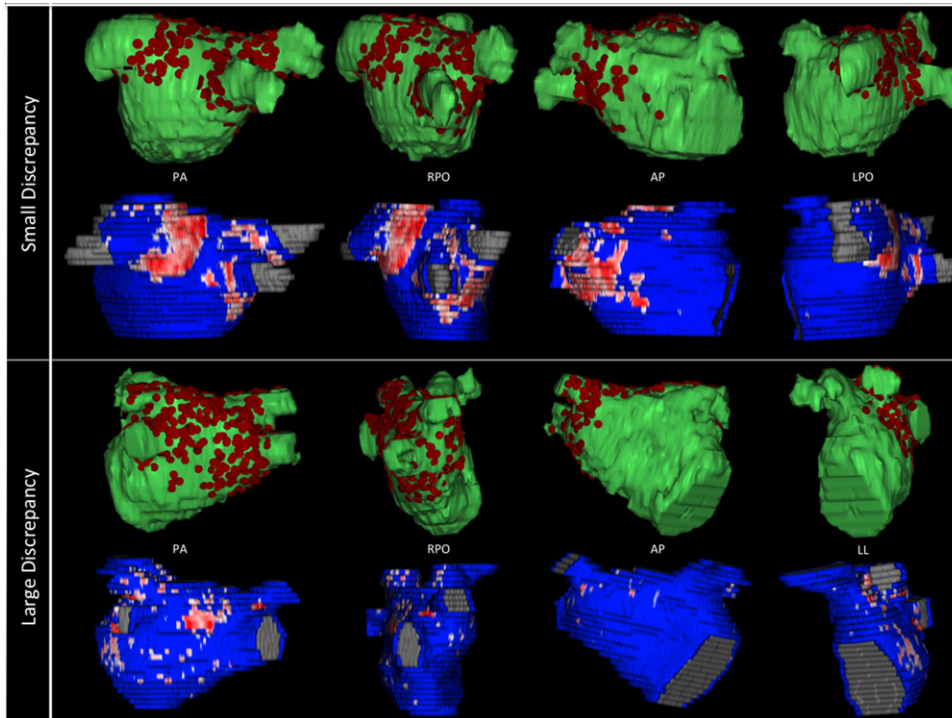
Figure 3. *Comparison of PVI in EAM and follow-up LGE-MRI in 2 patients. The upper rows show a close correlation between ablation tags marked in EAM (row 1) with corresponding scar in follow-up LGE-MRI (row 2). The difference between ablated and scarred areas was 5.3%. Rows 3 and 4 demonstrate a much greater difference (30.6%) between EAM and LGE-MRI areas. AP = anteroposterior; EAM = electroanatomic mapping; LGE-MRI = late-gadolinium enhancement magnetic resonance imaging; LL = left lateral; LPO = left posterior oblique; PA = posteroanterior; PVI = pulmonary vein isolation; RPO = right posterior oblique.*
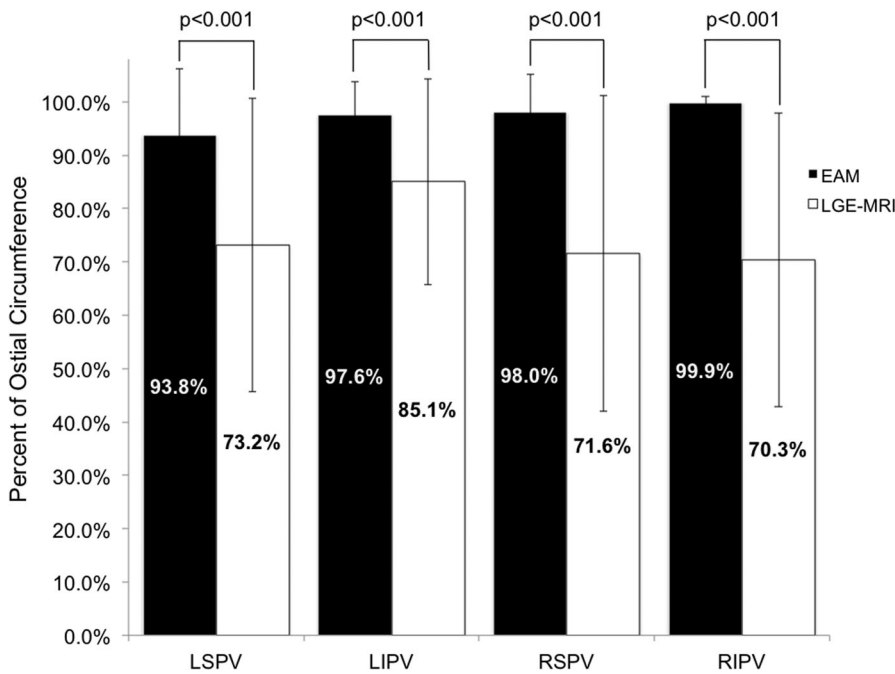

Figure 4. *Comparison of mean percent encirclement of each PV in EAM and scar from LGE-MRI (P values <0.001 for each PV comparison). EAM = electroanatomic mapping; LGE-MRI = late-gadolinium enhancement magnetic resonance imaging; LIPV = left inferior pulmonary vein; LSPV = left superior pulmonary vein; RIPV = right inferior pulmonary vein; RSPV = right superior pulmonary vein.*

patients with none of the veins marked isolated in EAM compared to 30% of patients in LGE-MRI.

In the subset of patients (n = 10), the ablation area was also measured using reduced ablation point tag size of 1 mm radius in EAM. The percent of LA wall area covered by 1 mm tags was $21.2 \pm 5.2\%$ and the percent of LA wall area covered by 2 mm tags in the same group of patients was 26.5 $\pm 8\%$. The percent of LA area covered by scar in this group of patients based on LGE-MRI was $12.0 \pm 5.1\%$. The mean ablated area in the EAM when using 1 mm radius tags was diminished compared to 2 mm radius tags, but the disparities between the ablated area in EAM and scar area seen in LGE-MRI remained significant (1 mm: P < 0.001; 2 mm: P < 0.001).

Figure 5. *Comparison of completely encircled PVs with ablation tags in EAM and scar in LGE-MRI. Complete encirclement defined as >90% encirclement of the PVs by ablation tags or scar. Differences were significant for all 4 vein pairs (P < 0.001). EAM = electroanatomic mapping; LGE-MRI = late-gadolinium enhancement magnetic resonance imaging; LIPV = left inferior pulmonary vein; LSPV = left superior pulmonary vein; RIPV = right inferior pulmonary vein; RSPV = right superior pulmonary vein.*
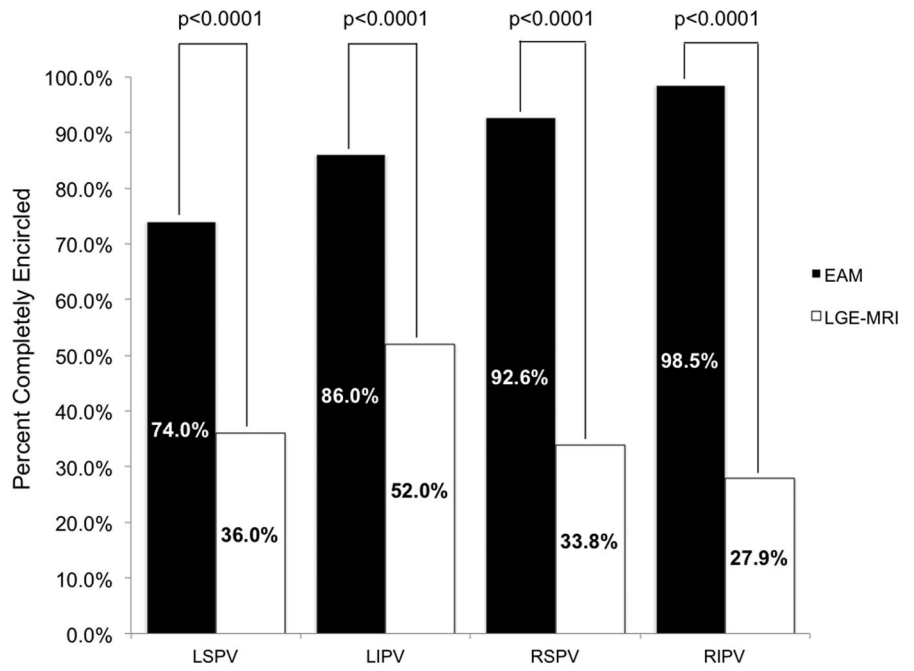
Figure 6. *Comparison of mean ablated area along with corresponding standard deviation in EAM and in LGE-MRI for each operator (P < 0.01). Means are presented in columns with standard deviation bars. EAM = electroanatomic mapping; LA = left atrium; LGE-MRI = late-gadolinium enhancement magnetic resonance imaging.*
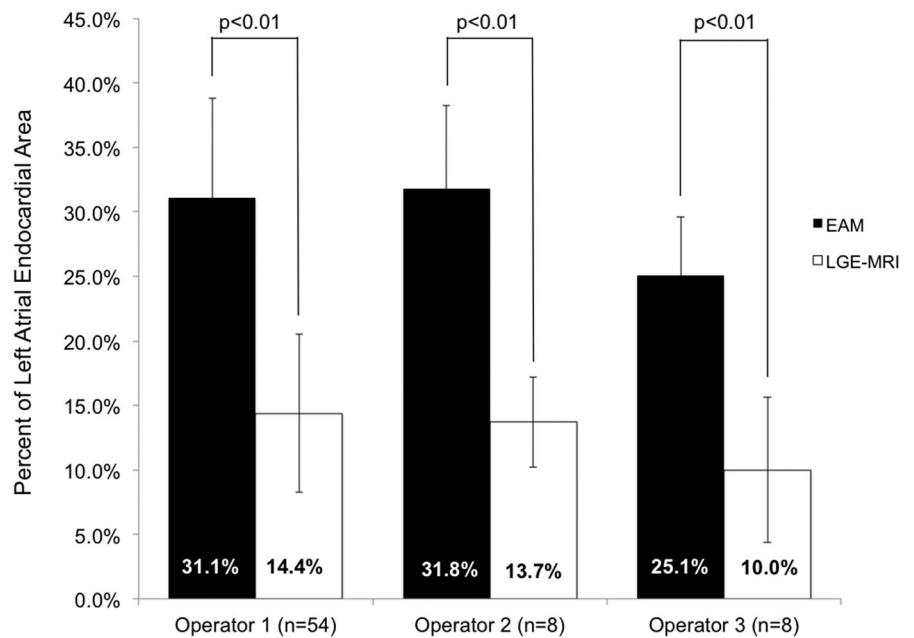
The differences between EAM ablation area and scar area on LGE-MRI persisted among all 3 operators (Fig. 6). Operators 1 and 2 had similar mean ablation areas in EAM of 31–32% and mean scar areas in LGE-MRI of 14%, whereas operator 3 had a lower mean ablation area in EAM of 25.1% and subsequently lower mean scar area on LGE-MRI of 10%. All differences between EAM and LGE-MRI were significant (P values <0.01). The total ablation time for all 3 operators was similar at 2,146 seconds for operator 1; 2,748 seconds for operator 2; and 2,957 seconds for operator 3.

Discussion

This study sought to evaluate correlations between the ablated areas marked in EAM during the procedure with resultant scar areas as determined by follow-up LGE-MRI.

One prior study has shown a relationship between the intended sites of ablation and LGE-MRI scar in 19 patients, and did not find scar at approximately 20% of the marked ablation sites upon follow-up.[11] This study elaborates upon that result and demonstrates that the intended area of ablation as marked on EAM significantly overestimates the actual scar on LGE-MRI across multiple operators and ablation tag sizes. Similarly, ablation tags on EAM that indicate complete or nearly complete encirclement of PV ostia by ablation correlate inconsistently with encirclement by scar in LGE-MRI. Quantitatively, the percent of PV encirclement with ablation tags was also overestimated in EAM when compared to the percent PV encirclement with scar in LGE-MRI (Fig. 4).

Our study also showed that this tendency of EAM to overestimate scar formation in LGE-MRI is not operator dependent but was found across 3 operators using

different ablation techniques with varying combinations of power and catheter movement. Despite these different techniques, the difference between ablation area in EAM and scar area on LGE-MRI was significant for all the 3 operators.

The observed differences between EAM ablated area and LGE-MRI scar could be explained in several ways: lack of proper contact between the LA tissue and the ablation catheter, inadequate time spent at the ablation site (or the frequency at which the tags are placed on the EAM), formation of transient edema at the ablation site that recovers over time, or the size of the tags marking ablation being much bigger than the area ablated.

The use of tags with 2 mm radius is the current standard across most centers and reasonably assumes the size of lesions created using catheters with a 3.5-mm tip.[15] Prior work looking at ablation lesions with similar size catheter tip has shown that even 5 W of power can create 5 mm size ventricular lesions and significantly larger lesions at higher power.[16] In this study, reducing the size of tags to mark the ablated area did reduce the calculated ablation area in the EAM but did not resolve the difference in area between EAM and LGE-MRI. Moreover, the size of ablation tags was reduced retrospectively during the time of the analysis, creating additional gaps in the ablation that contributed to decreased ablated area. Given that most operators prefer to create contiguous lesion sets in PV isolation, it is likely that use of 1 mm tags during the ablation procedure itself would result in these gaps being filled and an ablated area closer to that marked with 2 mm radius tags.

Adjusting ablation tag acquisition parameters based on catheter stability, wattage, temperature, or impedance change might also be effective in mapping ablated areas that will correlate more consistently with resultant scar areas. But as one gets more aggressive with ablation, one has to balance the increased risk of complications with more force or increased ablation time. In addition to the catheter-related features that impact ablation tag acquisition, the frequency with which tags are placed can make a big difference in the area deemed to be ablated. However, finding optimal frequency of tag placement is challenging given the large number of variables that factor into good lesion formation. In this study, we used the clinical maps created at the time of the ablation with the operator marking the spots deemed to be ablated based on well-accepted current clinical practice including elimination of local electrograms. Tagging areas as ablated after eliminating local electrograms is the current clinical practice but clearly seems to overestimate the area that will result in scar. A direct feedback of tissue changes, as ablation is carried out, can potentially help in narrowing this discrepancy.

The use of force sensing catheters can provide some indication of tip-to-tissue contact, but the lack of any direct feedback of tissue changes will persist as a central problem for electrophysiologists.[17,18] Furthermore, transmurality of lesions is dependent not only on good tissue contact but also on energy delivered, duration of the energy delivered, the catheter contact force, catheter tip area in contact with the tissue, and irrigated versus nonirrigated catheter tips. Given that acute electrical isolation of PVs confirmed with the Lasso catheter offers some evidence of encirclement of the PVs by lesions, the observed differences may stem from gaps in lesions sets with edema that contribute to acute isolation of

the veins but recover over time. The possibility of acute isolation despite the presence of gaps in lesion sets has been demonstrated both computationally and experimentally.[19]

MRI offers a promising avenue for resolving this discrepancy. MRI has excellent soft tissue characterization ability and has been used to acutely identify ablation-related tissue changes.[15,16] Using MRI to identify gaps in ablation lesions sets and target them is one potential way to bridge this gap between the marked area in EAM believed to be ablated and true scar as seen in LGE-MRI.[20,21] Even though a real-time MRI system seems to be a most promising method for direct visualization of changes to the tissue from ablation, limitations remain, and accurate determination of long-term scar from scans done acutely is still an area of active investigation.

Further work is needed to elucidate the observed discrepancies between EAM ablation and LGE-MRI scar. Prior studies have shown that smaller scar area on LGE-MRI correlates with higher AF recurrence.[9,10] For the first time, we show that large areas marked as ablated in the EAM do not result in long-term scar and could well be the reason for high recurrence rates of arrhythmias like AF. Further studies are needed to associate AF recurrence with the difference between EAM ablation area and LGE-MRI scar area to provide the necessary impetus to advocate for delivery of more effective lesions.

Conclusions

In AF ablation, EAM ablation mapping significantly overestimates scar formation when compared to LGE-MRI. Better visualization and ablation mapping techniques are necessary to achieve the desired LA scar.

Limitations

We acknowledge significant limitations to this study. This is a retrospective analysis of a single center, AF ablation population, although multiple operators with various ablation techniques were represented. Furthermore, variables derived from procedures may have significant inter- and intraobserver variability. To reduce interobserver variability, we derived a consensus from 2 blinded independent experts for EAM and 3 blinded independent reviewers for LGE-MRI to document PV encirclement as well as ablated and scarred areas. Also, this study does not make an attempt to predict areas marked as ablated in EAM that will result in scar or heal over time and if this difference between areas deemed ablated versus scar affects procedural outcome. Correlating this difference between areas deemed ablated in EAM and resulting scar with procedural outcome is needed before we make any changes to our ablation approach.

References

1. Haissaguerre M, Jais P, Shah DC, Takahashi A, Hocini M, Quiniou G, Garrigue S, Le Mouroux A, Le Metayer P, Clementy J: Spontaneous initiation of atrial fibrillation by ectopic beats originating in the pulmonary veins. N Engl J Med 1998;339:659-666.
2. Pappone C, Rosanio S, Oreto G, Tocchi M, Gugliotta F, Vicedomini G, Salvati A, Dicandia C, Mazzone P, Santinelli V, Gulletta S, Chierchia S: Circumferential radiofrequency ablation of pulmonary vein

ostia: A new anatomic approach for curing atrial fibrillation. Circulation 2000;102:2619-2628.

3. Segerson NM, Daccarett M, Badger TJ, Shabaan A, Akoum N, Fish EN, Rao S, Burgon NS, Adjei-Poku Y, Kholmovski E, Vijayakumar S, Di Bella EV, MacLeod RS, Marrouche NF: Magnetic resonance imaging-confirmed ablative debulking of the left atrial posterior wall and septum for treatment of persistent atrial fibrillation: Rationale and initial experience. J Cardiovasc Electrophysiol 2010;21:126-132.

4. Malchano ZJ, Neuzil P, Cury RC, Holmvang G, Weichet J, Schmidt EJ, Ruskin JN, Reddy VY: Integration of cardiac CT/MR imaging with three-dimensional electroanatomical mapping to guide catheter manipulation in the left atrium: Implications for catheter ablation of atrial fibrillation. J Cardiovasc Electrophysiol 2006;17:1221-1229.

5. Peters DC, Wylie JV, Hauser TH, Kissinger KV, Botnar RM, Essebag V, Josephson ME, Manning WJ: Detection of pulmonary vein and left atrial scar after catheter ablation with three-dimensional navigator-gated delayed enhancement MR imaging: Initial experience. Radiology 2007;243:690-695.

6. Hunter RJ, Jones DA, Boubertakh R, Malcolme-Lawes LC, Kanagaratnam P, Juli CF, Davies DW, Peters NS, Baker V, Earley MJ, Sporton S, Davies LC, Westwood M, Petersen SE, Schilling RJ: Diagnostic accuracy of cardiac magnetic resonance imaging in the detection and characterization of left atrial catheter ablation lesions: A multicenter experience. J Cardiovasc Electrophysiol 2013;24:396-403.

7. Badger TJ, Daccarett M, Akoum NW, Adjei-Poku YA, Burgon NS, Haslam TS, Kalvaitis S, Kuppahally S, Vergara G, McMullen L, Anderson PA, Kholmovski E, MacLeod RS, Marrouche NF: Evaluation of left atrial lesions after initial and repeat atrial fibrillation ablation: Lessons learned from delayed-enhancement MRI in repeat ablation procedures. Circ Arrhythm Electrophysiol 2010;3:249-259.

8. McGann C, Kholmovski E, Blauer J, Vijayakumar S, Haslam T, Cates J, DiBella E, Burgon N, Wilson B, Alexander A, Prastawa M, Daccarett M, Vergara G, Akoum N, Parker D, MacLeod R, Marrouche N: Dark regions of no-reflow on late gadolinium enhancement magnetic resonance imaging result in scar formation after atrial fibrillation ablation. J Am Coll Cardiol 2011;58:177-185.

9. McGann CJ, Kholmovski EG, Oakes RS, Blauer JJ, Daccarett M, Segerson N, Airey KJ, Akoum N, Fish E, Badger TJ, Di Bella EV, Parker D, MacLeod RS, Marrouche NF: New magnetic resonance imaging-based method for defining the extent of left atrial wall injury after the ablation of atrial fibrillation. J Am Coll Cardiol 2008;52:1263-1271.

10. Peters DC, Wylie JV, Hauser TH, Nezafat R, Han Y, Woo JJ, Taclas J, Kissinger KV, Goddu B, Josephson ME, Manning WJ: Recurrence of atrial fibrillation correlates with the extent of post-procedural late gadolinium enhancement: A pilot study. JACC Cardiovasc Imaging 2009;2:308-316.

11. Taclas JE, Nezafat R, Wylie JV, Josephson ME, Hsing J, Manning WJ, Peters DC: Relationship between intended sites of RF ablation and post-procedural scar in AF patients, using late gadolinium enhancement cardiovascular magnetic resonance. Heart Rhythm 2010;7:489-496.

12. Vergara GR, Marrouche NF: Tailored management of atrial fibrillation using a LGE-MRI based model: From the clinic to the electrophysiology laboratory. J Cardiovasc Electrophysiol 2010;22:481-487.

13. Badger TJ, Oakes RS, Daccarett M, Burgon NS, Akoum N, Fish EN, Blauer JJ, Rao SN, Adjei-Poku Y, Kholmovski EG, Vijayakumar S, Di Bella EV, MacLeod RS, Marrouche NF: Temporal left atrial lesion formation after ablation of atrial fibrillation. Heart Rhythm 2009;6:161-168.

14. Ranjan R: Magnetic resonance imaging in clinical cardiac electrophysiology. Crit Rev Biomed Eng 2012;40:409-426.

15. Dickfeld T, Kato R, Zviman M, Lai S, Meininger G, Lardo AC, Roguin A, Blumke D, Berger R, Calkins H, Halperin H: Characterization of radiofrequency ablation lesions with gadolinium-enhanced cardiovascular magnetic resonance imaging. J Am Coll Cardiol 2006;47:370-378.

16. Dickfeld T, Kato R, Zviman M, Nazarian S, Dong J, Ashikaga H, Lardo AC, Berger RD, Calkins H, Halperin H: Characterization of acute and subacute radiofrequency ablation lesions with nonenhanced magnetic resonance imaging. Heart Rhythm 2007;4:208-214.

17. Kuck KH, Reddy VY, Schmidt B, Natale A, Neuzil P, Saoudi N, Kautzner J, Herrera C, Hindricks G, Jais P, Nakagawa H, Lambert H, Shah DC: A novel radiofrequency ablation catheter using contact force sensing: Toccata study. Heart Rhythm 2012;9:18-23.

18. Reddy VY, Shah D, Kautzner J, Schmidt B, Saoudi N, Herrera C, Jais P, Hindricks G, Peichl P, Yulzari A, Lambert H, Neuzil P, Natale A, Kuck KH: The relationship between contact force and clinical outcome during radiofrequency catheter ablation of atrial fibrillation in the Toccata study. Heart Rhythm 2012;9:1789-1795.

19. Ranjan R, Kato R, Zviman MM, Dickfeld TM, Roguin A, Berger RD, Tomaselli GF, Halperin HR: Gaps in the ablation line as a potential cause of recovery from electrical isolation and their visualization using MRI. Circ Arrhythm Electrophysiol 2011;4:279-286.

20. Lardo AC, McVeigh ER, Jumrussirikul P, Berger RD, Calkins H, Lima J, Halperin HR: Visualization and temporal/spatial characterization of cardiac radiofrequency ablation lesions using magnetic resonance imaging. Circulation 2000;102:698-705.

21. Ranjan R, Kholmovski EG, Blauer J, Vijayakumar S, Volland NA, Salama ME, Parker DL, MacLeod R, Marrouche NF: Identification and acute targeting of gaps in atrial ablation lesion sets using a real-time magnetic resonance imaging system. Circ Arrhythm Electrophysiol 2012;5:1130-1135.